Membrane separation of porcine blood for food industrial use of permeate and retentate

TAMÁS CSURKA – ÁRON VARGA – MÁRTA LADÁNYI – LÁSZLÓ FERENC FRIEDRICH – KLÁRA PÁSZTOR-HUSZÁR

Summary

In this article, we introduce the importance of blood processing for human consumption while also presenting the methodology of porcine blood membrane separation to plasma and red blood cell fractions, as well as the membrane purification after porcine blood separation. Basic analytical measurements were carried out to investigate the blood product attributes, which relate to technological and nutritional quality depending on the separation parameters. Next, we present how the relevant hydrodynamical parameters were calculated during the experiments. Membrane separation was realized by crossflow microfiltration with pore size of 0.8 μm or 1.2 μm, retentate flow rate of 200 $l \cdot h^{-1}$ or 300 $l \cdot h^{-1}$ and with transmembrane pressure of 1×10^5 Pa, 2×10^5 Pa or 3×10^5 Pa. The experimental design was analysed, the parameters of the objective function and effect sizes were estimated and the global minimum of the objective function was successfully identified. The results of this optimization can be applied in practice. The membrane separation parameters were then optimized according to a model based on the observed data. An optimum was detected within the examined factor levels and experimental conditions at the lowest transmembrane pressure and at the highest membrane pore size.

Keywords

animal blood; blood separation; by-product; membrane technology; microfiltration; sustainability

Sustainability and utilization of by-products are hot spots of scientific literature since consumers prefer a sustainable food system [1]. There are three major arguments for the incorporation of animal by-products to the highest extent possible, for instance, to substitute meat. The first argument is the need to increase competitiveness of the meat industry and to reduce the "carbon footprint" of livestock [2], which is estimated to represent 14.5 % of human-induced greenhouse gas emission [3]. Absolute and relative overpopulation is taken as the second argument, as the absolute population of 9×10^9 or more people is predicted for 2050 [4]. Relative overpopulation means, in this case, a larger meat demand growth than the population growth. While the Earth's population doubled between 1950 and 2000, the volume of meat production increased nearly five-fold, yearly from 45×10^6 t to 233×10^6 t [5]. Meanwhile the infield area, 1.6×10^{13} m^2 in 2016 can be expanded to a maximum of 1.8×10^{13} m^2 [4]. 58×10^6 t protein is consumed by humans from the produced 77×10^6 t protein in a year [6], while near 11 % of population (7.95×10^8 people)

Tamás Csurka, Department of Livestock Products and Food Preservation Technology, Institute of Food Science and Technology, Hungarian University of Agriculture and Life Sciences, Ménesi str. 43–45, H-1118 Budapest, Hungary; Doctoral School of Food Sciences, Hungarian University of Agriculture and Life Sciences, Villányi str. 29–43, H-1118 Budapest, Hungary.
László Ferenc Friedrich, Klára Pásztor-Huszár, Department of Livestock Products and Food Preservation Technology, Institute of Food Science and Technology, Hungarian University of Agriculture and Life Sciences, Ménesi str. 43–45, H-1118 Budapest, Hungary.
Áron Varga, Doctoral School of Food Sciences, Hungarian University of Agriculture and Life Sciences, Villányi str. 29–43, H-1118 Budapest, Hungary.
Márta Ladányi, Department of Applied Statistics, Institute of Mathematics and Basic Science, Hungarian University of Agriculture and Life Sciences, Villányi str. 29–43, H-1118 Budapest, Hungary.

Correspondence author:
Tamás Csurka, e-mail: csurka.tamas@uni-mate.hu

are starving [7]. Besides, 1.6×10^9 people in the world are anemic, children suffering from iron deficiency anemia at a very high rate [8]. A portion of 100 g porcine blood powder can cover the daily essential amino acid need of an adult weighing 70 kg, but it is unable to satisfy his or her methionine needs [9]. Porcine blood contains 1 490.14 $mg \cdot kg^{-1}$ iron in dry mass [10] and bovine blood contains 2 810.62 $mg \cdot kg^{-1}$ iron in dry mass according to the USDA National Nutrient Database for Standard Reference [11], which is outstanding among food ingredients. Moreover, the absorption of hem iron in human body is better than other forms of iron [12]. Animal blood could be a perfect raw material, not only for functional food but also for common food production [13–15]. Another reason for utilizing animal blood is the third argument, specifically, its high environmental pollution capabilities. As blood is classified as hazardous waste, it requires appropriate handling dictated by strict regulations such as regulation (EC) No. 853/2004 on specific hygiene rules for food of animal origin [16]. The biological and chemical oxygen demand of blood [13] exceed the limiting value of polluting power of hazardous wastes. The COVID-19 pandemic crisis caused significant challenges in the food industry, which made it necessary to reduce losses and food waste as well as identifying alternative and safe protein sources to make our food systems more sustainable and resilient to increase food security [17].

Functional foods are acceptable and economically competitive products, which can be enriched with, for instance, blood products like hem-iron, protein (with good gelling and foaming capacity) and bioactive peptides [18–21]. Valorization of a vast range of bioresources for instance by biorefining or innovations in the field of sustainability (e. g. laboratory-grown aseptic meat, plant-based meat alternatives, biobased packaging, automation of food production or robotics) is more important than ever after the COVID-19 pandemic crisis, instead of the traditional approaches for managing food waste including land-filling and incineration [22].

Certain blood-containing foods are available in several countries but these are sought just by a narrow segment of consumers because of the typical sensory attributes. More uses may be possible after the blood is separated and the blood products are handled separately. But before the separation blood coagulation, which changes the blood sol state that is well suited for further processing to gel state, has to be inhibited. Trisodium citrate affects factor IV (i. e. calcium) from the 13 blood-clotting factors preventing the change in blood texture. The group of sodium citrates is an approved food additive E 331, which may be used in prepared meat products without quantitative restrictions according to regulation (EC) No 1333/2008 on food additives [23].

Plasma in a share of 520–700 $g \cdot kg^{-1}$ of whole blood mass is produced during the separation of whole blood, depending on the technology and requirements of the products [9]. Plasma does not contain blood cells. It is not red and has no metallic taste and smell like blood. Blood plasma can be decolourized by chemical treatment and extraction of the residual hemoglobin, afterwards obtaining a tea-like colour [24]. It is ideal for increasing the protein content of foods or for developing food texture without significant taste, smell and colour changes. The low lipid content of plasma and opportunity of application at lipid uptake reduction have to be mentioned because of the fact that obesity rates have reached a staggering number worldwide [25].

By separation of whole blood, red blood cell fraction in a share of 300–480 $g \cdot kg^{-1}$ of whole blood is produced, depending on the technology and requirements of the products [9]. The red blood cell fraction got its name from red blood cells forming the largest part of this fraction, but it contains also some other blood cells. It gets a deep black colour with strong iron taste as a result of heat treatment. It can be a raw material for functional or other specific food types without any further processing.

Centrifugal separation is being developed continuously but, in certain cases, membrane technology may be more efficient than centrifugation. Moreover, membrane technology can be made more selective than centrifugation, especially if membranes are combined with magnetic field or a special pore size is used. Thus, blood products may be more suitable for various purposes. Blood is a perishable material, which can easily become a substrate for harmful microorganisms, thus, cleaning of membranes is crucial to avoid contamination. Inorganic (e. g. ceramic) membranes are generally used for filtration because they show very good thermal and chemical stability and can be cleaned aggressively (e. g. by steam and strong acid or alkali) and used in industry under harsh conditions [26]. The disadvantages of membrane separation are the relatively high installation cost and limited experience. However, clear advantages over conventional technologies are good controllability, as well as efficiency may be better too besides the adequate blood volume.

The application of compounds recovered from food processing by-products and eco-friendly (e. g. non-thermal) technologies can increase profit

and secure sustainable development of the food industry [27].

MATERIAL AND METHODS

Blood

Porcine blood was collected manually in Hungary in a slaughterhouse directly from the slaughtered pork during bloodletting. Breed of pigs (*Sus scrofa domesticus*) were mangalica × duroc hybrid, duroc and Hungarian landrace. Trisodium citrate was used to prevent blood coagulation. Dry trisodium citrate dihydrate powder (Reanal Laborvegyszer, Budapest, Hungary) was added to the blood directly after collection to 5 $g \cdot kg^{-1}$, for keeping the filterable state, and then the substances were mixed well. The blood was stored at 0–2 °C without freezing until the membrane separation process (for 1–4 days).

Membranes

Tubular, one-channel ceramic membranes (Atech Innovations, Gladbeck, Germany) with an active layer of aluminium oxide were used. The outer diameter of the membranes was 10.0 mm, the inner diameter of the membranes was 6.0 mm. The specific membrane area of membranes, which means the filtering surface in the specification of the producer, was 0.019 $m^2 \cdot m^{-1}$ and the length of membranes was 250 mm (whole filter surface per element was approximately 0.00475 m^2). The membranes were suitable for steam sterilization above 121 °C and acidic and basic material filtration at pH 0–14. All re-usable and corrosion-resistant tools and equipment were multi-phase cleaned with sodium hypochlorite and a detergent. Citric acid monohydrate (Reanal Laborvegyszer) and sodium hydroxide flakes (Sigma Aldrich, St. Louis, Missouri, USA) were used for membrane cleaning.

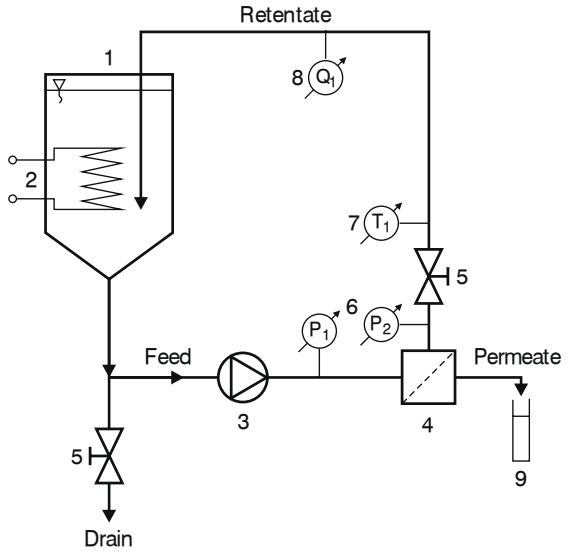

Fig. 1. Schematic flow diagram of bench-scale cross-flow microfiltration equipment.

1 – feed tank, 2 – heat exchanger (cooler/heater), 3 – pump, 4 – microfiltration membrane module, 5 – valve, 6 – manometres, 7 – thermometer, 8 – flowmeter, 9 – measuring cylinder.
P_1 – pressure measured in the pipe before the membrane, P_2 – pressure measured in the pipe after the membrane, T_1 – temperature measured in the pipe, Q_1 – measured retentate flow rate.

Microfiltration

In this investigation, membrane microfiltration, as a separation method, was evaluated. The crossflow microfiltration equipment (Fig. 1) was developed at the Department of Food Engineering, Hungarian University of Agriculture and Life Sciences (Budapest, Hungary). The factors of the experiment were set as: pore size (0.8 μm, 1.2 μm), retentate flow rate (200 $l \cdot h^{-1}$, 300 $l \cdot h^{-1}$) and transmembrane pressure (1×10^5 Pa, 2×10^5 Pa, 3×10^5 Pa). Factor levels were selected according to preliminary tests, considering the experiment duration to the steady-state phase and the quality of blood fractions. Samples were collected from feed (whole blood), permeate (blood plasma) and retentate (red blood cells) for convenient characterization of raw material and products. Permeate samples were collected during the entire filtration time except for the first 5 ml because of residual water in the permeate pipe. Initially, the temperature was 5 °C and was increased to various final temperature values (10–20 °C) despite the cooling (heat exchanger set to 5 °C in the feeding tank and controlled room temperature set to 15 °C) during the filtration. Pressure at both ends of the membrane, temperature at the pipe and in the feed tank, blood flux and retentate flow (using the pump data) were measured. The sampling and data recording frequency was 0.5 min during the first 20.5 min and then 1 min until the end of the filtration. A volume of 80 ml of the permeate was collected from each experiment. The duration of the filtration depended on the flux. The membranes and the entire piping system were cleaned before and after each filtration. Water flux was measured before each filtration. Water was drained with the valve at the bottom after water flux measurement to avoid dilution of whole blood. Residual water was removed by mixing whole blood from the piping system with a pump.

Experimental settings are shown in Tab. 1. The experiments were performed in random order, the set numbers of experiments are not related to the order of performance.

Tab. 1. Experimental setups.

Designation	*TMP* [Pa]	Retentate flow [l·h^{-1}]	Membrane pore size [μm]
01	1×10^5	200	0.8
02	1×10^5	200	1.2
03	1×10^5	300	0.8
04	1×10^5	300	1.2
05	2×10^5	200	0.8
06	2×10^5	200	1.2
07	2×10^5	300	0.8
08	2×10^5	300	1.2
09	3×10^5	200	0.8
10	3×10^5	200	1.2
11	3×10^5	300	0.8
12	3×10^5	300	1.2

TMP – transmembrane pressure.

Membrane cleaning

A series of experiments led us to find a suitable cleaning method in case of porcine blood microfiltration. A relatively aggressive cleaning procedure was required because of the extreme contamination and pores clogging by blood components that swelled due to the pH change. The cleaning process of the equipment was limited by its sensitivity to extreme pH and temperature, as well as to corrosion of the membrane pump and pressure sensors.

This cleaning process was performed by:

1. rinsing with water and then 30 min cleaning with water at room temperature (20 °C),
2. 30 min cleaning with 1% sodium hydroxide at 60 °C and then rinsing with water,
3. 30 min cleaning with water at room temperature (20 °C),
4. 30 min cleaning with 1% citric acid at 60 °C and then rinsing with water,
5. 30 min cleaning with water at room temperature (20 °C).

In addition, the membranes needed a more aggressive cleaning outside the equipment. This cleaning process was performed by:

1. 30 min soaking in water at 80 °C,
2. 30 min cleaning with 10% sodium hydroxide at 80 °C,
3. 30 min cleaning with water at 80 °C,
4. 30 min cleaning with 10% sodium hypochlorite at 80 °C,
5. rinsing with water and soaking in water at room temperature (20 °C) until the next filtration (for 8 h).

The membranes were conditioned for 45 min in the equipment with water for stable water flux.

Rheological measurements

Physica MCR 91 viscometer (Anton-Paar, Ostfildern, Germany) was used for rheological measurements. The behaviour of samples (especially theoretical viscosity) was measured under variable speed shear stress with concentric cylinders (CC27) by Couette-type method. A number of 2 × 31 data were collected during one measurement run. The revolutions per minute (RPM) of the inner cylinder varied between 1 min^{-1} and 1 000 min^{-1}. The outcome of the measurement was a flow curve, to which a model was fitted. This model can define the rheological behaviour of the samples and the rheological parameters can be calculated following calibration of the model. The flow behaviour of all samples could be described by the Herschel-Bulkley model [28] considering the following parameters: shear stress (τ), theoretical yield point (τ_0), deformation speed (γ), consistency index (C) and power of law index (p). A new shear rate was calculated from these parameters and this new shear rate validated the compliance of the model. The determination coefficient (R^2) that describes the explained variance rate indicated a highly significant model with its values greater than 0.9965 in case of all samples. Measurements of permeates and retentates were carried out at 5 °C, 12.5 °C and 20 °C to correct the error caused by changes in temperature that were experienced during the membrane filtration. Each sample was measured in triplicate.

Colour measurement

Minolta CR-400 (Konica Minolta, Tokyo, Japan) colorimeter was used for reflectional colour measurement. In case of blood, there is a relation between the red colour (and chroma) and the iron content, hereby between the physical and chemical attributes. Each sample was measured in triplicate. The measured attributes were redness/greenness (a^*), yellowness/blueness (b^*), brightness (L^*) and from these, chroma (C^*) was calculated using Eq. 1 [29]:

$$C^* = \sqrt{a^{*2} + b^{*2}} \quad (1)$$

Water activity measurement

Water activity was measured by LabMaster-aw neo type water activity measurement device (Novasina, Lachen, Switzerland). Measurements were performed at room temperature (20 °C) to control the integrity of samples for relevant data detection. Each sample was measured in triplicate.

Dry matter measurement

Amounts of 3–5 g sample were measured by ABJ-NM/ABS-N analytical balance (Kern & Sohn, Balingen, Germany). Then samples were put into a laboratory drying oven (Labor Műszeripari Művek, Budapest, Hungary) and were dried at 105 °C until they reached the state of constant mass. Samples were cooled in a desiccator and then their mass was measured by analytical balance. Each sample was measured in triplicate.

pH measurement

Voltcraft PHT-02 ATC pH stick (Conrad Electronic, Hirschau, Germany) was used for pH measurement. The principle of pH sticks operation is based on electronic differentiation between a referent electrode with a stable value and a pH-sensitive electrode in a fluid with any standard redox potential. Sample pH is calculated from the potential difference according to a linear correlation. The device was calibrated before each measurement series with two standard liquid samples. Each sample was measured in triplicate.

Hydrodynamic parameters determination

The viscosity of Herschel-Bulkley fluid flowing in a tube system depends on its temperature and shear stress affecting the fluid, therefore the shear stress needed to be calculated. Theoretical viscosity was measured under the calculated shear stress at three temperatures. A linear regression was fitted to these three points by Excel 365 (Microsoft, Redmond, Washington, USA) and then practical viscosity of the flowing fluid at the temperature measured during the filtration was interpolated.

The following interrelations were applied for calculating the filtration efficacy: In case of fluid flow in a round cross-section pipe, the shear stress at laminar flow can be expressed as Eq. 2:

$$\tau = \frac{f \times \nu^2 \times \rho}{8} \tag{2}$$

where τ is shear stress, f is resistance friction coefficient, ν^2 is squared retentate flow velocity, ρ is density of the fluid and number 8 is a constant in case of round cross-section pipe and laminar flow.

Equations about flow in a tube or pipe can be derived from the Navier-Stokes formula. It was assumed that laminar flow would be the basis of the experimental conditions and it was finally verified by the calculated results. Value of Reynolds number was 1 370.15 ± 568.32 during all experiments. Resistance friction coefficient (f) of pipe flow was calculated by Eq. 3:

$$f = \frac{A}{Re^d} \tag{3}$$

where A is the membrane inner cross section and d is the constant characterizing the flow (in case of laminar flow $A = 64$ and $d = 1$). Reynolds number (Re) can be calculated by Eq. 4:

$$Re = \frac{D_e \times \nu \times \rho_b}{\mu_b} \tag{4}$$

where D_e is the equivalent diameter of a round cross-section pipe, ν is retentate flow velocity, ρ_b is blood density and μ_b is blood viscosity. Shear stress (τ) of pipe flow was calculated by Eq. 5:

$$\tau = \frac{8 \times \mu_b \times \nu}{D_e} \tag{5}$$

Besides the equation for shear stress (τ), there is another equation from the applied and verified Herschel-Bulkley model for rheological measurements [28]:

$$\tau = \tau_0 + C \times \gamma^p \tag{6}$$

where τ_0 is theoretical yield point, C is consistency index, γ is deformation speed and p is power of law index.

If the data are substituted in the two simplified equations regarding shear stress, there remains only one unknown parameter except for viscosity, namely, shear stress. The following equations, by which shear stress can be determined for non-Newtonian fluids flow in a round cross-section pipe, can be derived from the Hagen-Poiseuille formula, which is described by Eq. 7 [28]:

$$\gamma = \frac{4 \times \nu}{\pi \times \left(\frac{D}{2}\right)^3} \tag{7}$$

where ν is retentate flow velocity, D is diameter of round cross-section pipe and denominator represents the calculation with a round cross-section pipe. Thereby, viscosity of each sample can be calculated at the filtration temperature with the set volume of retentate flow rate in our experimental equipment.

Efficiency of microfiltration was expressed by the calculated practical dynamic viscosity of blood flow in the piping system. Filtration efficiency can

be defined by the energy consumption calculated from permeate flux, which is the amount of permeate that is given on unit of filter surface per unit of time. It is described by Eq. 8 [30]:

$$J = \frac{V_i}{A_m \times t_i} \tag{8}$$

where J is flux, V_i is permeate volume during a time interval, A_m is the membrane active surface area and t_i is the time interval.

Flux was measured for steady-state blood microfiltration and for water. Energy consumption can be described by Eq. 9 [31]:

$$E_{ss} = \frac{P_{ss}}{A_m \times J_{b,ss}} \tag{9}$$

where E_{ss} is steady-state specific energy consumption, P_{ss} is steady-state hydraulic dissipation power, A_m is the membrane active surface area, and $J_{b,ss}$ is steady-state blood flux. The hydraulic dissipation power can be described by Eq. 10 [31]:

$$P_{ss} = Q_{ss} \times \Delta p \tag{10}$$

where Q_{ss} is steady-state retentate flow rate and Δp is the pressure drop along the membrane.

The intrinsic resistance of clean membrane (R_m) can be calculated from the viscosity of water (μ_w), water flux (J_w) and transmembrane pressure (TMP) by Eq. 11 [32]:

$$J_w = \frac{TMP}{\mu_w \times R_m} \tag{11}$$

and steady-state total resistance ($R_{t,ss}$) can be calculated from viscosity of whole blood (μ_b), steady-state blood flux ($J_{b,ss}$) and transmembrane pressure (TMP) by Eq. 12 [32]:

$$J_{b,ss} = \frac{TMP}{\mu_b \times R_{t,ss}} \tag{12}$$

The steady-state fouling layer total resistance ($R_{t,ss}$) value is the sum of intrinsic resistance of clean membrane resistance (R_m) and the steady-state fouling layer resistance ($R_{f,ss}$). It is described by Eq. 13 [33]:

$$R_{t,ss} = R_m + R_{f,ss} \tag{13}$$

The steady-state fouling layer resistance ($R_{f,ss}$) is an important parameter for planning an industrial blood membrane separator.

The cleaning efficacy was defined by flux recovery (FR) with the ratio of clean membrane resistance (R_m) and intrinsic resistance of the membrane after membrane cleaning (R_n) according to Eq. 14 [33]. FR is expressed in percent.

$$FR = \frac{R_m}{R_n} \times 100 \tag{14}$$

to which R_n can be described by Eq. 15 [33]:

$$J_{ww} = \frac{TMP}{\mu_w \times R_n} \tag{15}$$

where variables are the same as in Eq. 11.

Statistical evaluation

Measurement results were evaluated by IBM SPSS v. 25 (IBM, Armonk, New York, USA) and Excel 365 software. Excel was used for fitting the rheological model, correlation analysis, representation and performing mathematical operations. Determination coefficient (R^2) was evaluated. To detect the effect of transmembrane pressure, retentate flow rate and membrane pore size on redness/greenness (a^*), chroma (C^*) and dry matter content, multivariate analysis of variance (MANOVA) was carried out. According to Levene's test, the homogenity of variances was slightly violated ($p < 0.05$). The normality of residuals was checked by d'Agostino's test, providing a value of $p > 0.04$. The value of the unexplained variance rate (Wilks's lambda) was evaluated. In case of a significant overall MANOVA result, univariate follow-up ANOVA was run by Bonferroni's adjustment. The homogenous groups were separated by Games-Howell's post hoc test, which can manage inhomogenity of variances.

Modelling of hydrodynamical parameters

The research plan was based on a 2 × 2 × 3 full factorial experimental design. The aims of the application of this experimental design were to formulate an objective function describing the relationship between the dependent and independent variables, as well as to determine the significant parameters and the effect sizes. Response (Y) in this experimental design can be described by Eq. 16 [34]:

$$Y = b_0 + \sum_{i=1}^{3} b_i x_i + \sum_{i=1}^{3} \sum_{j=1, i \neq j}^{3} b_{ij} x_i x_j + \\ + b_{123} x_1 x_2 x_3 \tag{16}$$

where b_0 is the constant, b_i ($i = 1, 2, 3$) are regression coefficients of the main factor effects, b_{ij} ($i = 1, 2, 3$; $j = 1, 2, 3$; i ≠ j) and b_{123} are the regression coefficients of the interactions, x_i ($i = 1, 2, 3$) are the coded factors.

The most important hydrodynamic parameter is steady-state blood flux because this flux can generally affect the filtration during most

of the filtration time. However, the fouling characteristics are more accurately described by steady-state fouling layer resistance [35]. For this reason, steady-state fouling layer resistance was considered as the response of the applied full factorial experimental design.

The results of the experimental design were analysed in various steps by R studio software with package 'rsm' (R Core Team, R-3.5.1, R Foundation for Statistical Computing, Vienna, Austria) [36]. Criterions of modelling methods were checked, the residuals were normally distributed according to the Shapiro-Wilk normality test ($W = 0.87$; $p = 0.074$). The parameters of the objective function were estimated and the model accuracy and determination coefficients were evaluated. The insignificant parameter was eliminated from the model: The final model was built with the pore size and transmembrane pressure, without retentate flow rate. Then, the effect sizes of the significant parameters were calculated as well as model accuracy and determination coefficients were evaluated.

Limitations

Pigs were chosen as the starting livestock of blood separation because they are slaughtered in largest numbers from mammalian slaughter animals that can be bled safely. The whole blood, which was the feed of the microfiltration experiments, came from three blood collecting time points with three ratios of pig breeds since East-European slaughterhouses usually slaughter several pig populations each day. Besides breed, the quality of most livestock depends on season, forage quality and farming type.

The whole blood was stored at 0–2 °C for various times (1–4 days) before the experiment, because one experimental phase with membrane cleaning and water flux measuring took one whole day. Blood cannot be frozen because integrity of ingredients may change due to crystallization. The effect of the duration of storage could not be investigated but the experiments were performed in random order. Thus, if storage time was a randomised independent variable, the effect of storage time was compensated.

RESULTS AND DISCUSSION

Analysis of whole blood and blood fractions

Membrane separation was considered to be globally successful as the average dry matter content of plasma fell below 50 $g \cdot kg^{-1}$, the average water activity of plasma was above 0.96 and the average L^*, the brightness of plasma was above 25. Besides, in case of the red blood cell fraction, dry matter content was approximately 200 $g \cdot kg^{-1}$, like in the case of whole blood, water activity was 0.95–0.99, which was nearly the same as the value of whole blood (0.95–0.99), and the average L^* was 23.6, which was also similar to the value of whole blood (23.4). All water activity values for whole blood, plasma and red blood cell fraction were between 0.95 and 1. In every case, these products must be concentrated and/or dried or immediately processed. pH values of whole blood were 7.23–7.80, of plasma fraction 8.2–8.79 and of red blood cell fraction 7.30–7.77. Because the quality of whole blood feed varied, as in the practice of conventional Central and Eastern European slaughterhouses, the quality of separation can be indicated in many attributes by the difference between the attributes of plasma and red blood cell fractions. For instance, pH difference can indicate the appropriateness of separation of protein fraction. This pH difference was similar in case of experiments with the same retentate flow rate and transmembrane pressure. So, membrane pore size did not affect protein separation as strongly as the other two factors. In case of dry matter content, results were interesting. Due to high transmembrane pressure, cells were broken and dry matter content of plasma and red blood cell fractions were closer to each other than in case of lower transmembrane pressures. Additionally, bigger membrane pore size (1.2 μm) redounded greater difference between dry matter content of two blood product (21.1 %, 18.8 %, 22.7 %, 18.7 %) beside lower transmembrane pressure (1×10^5 Pa, 2×10^5 Pa), and the same pore size (1.2 μm) redounded smaller difference between dry matter content of two blood product (17.7 %, 17.6 %) beside higher transmembrane pressure (3×10^5 Pa). This can be explained by the formation of fouling layer, which took place slower if cells and aggregates could pass through pores without high pressure, which clogged the pores with bigger aggregates. The measured blood quality attributes (in opposite to the hydrodynamic parameters) were influenced not only by the transmembrane pressure and the membrane pore size, but also by the retentate flow.

These trend-like results could be observed but a linear model could not be generated on most of the measured attributes. Significant effects and differences between sample groups were evaluated by MANOVA. The overall MANOVA result was significant for transmembrane pressure, retentate flow rate and membrane pore size (Wilks's lambda values of 0.07, 0.04 and 0.44, respectively, all with

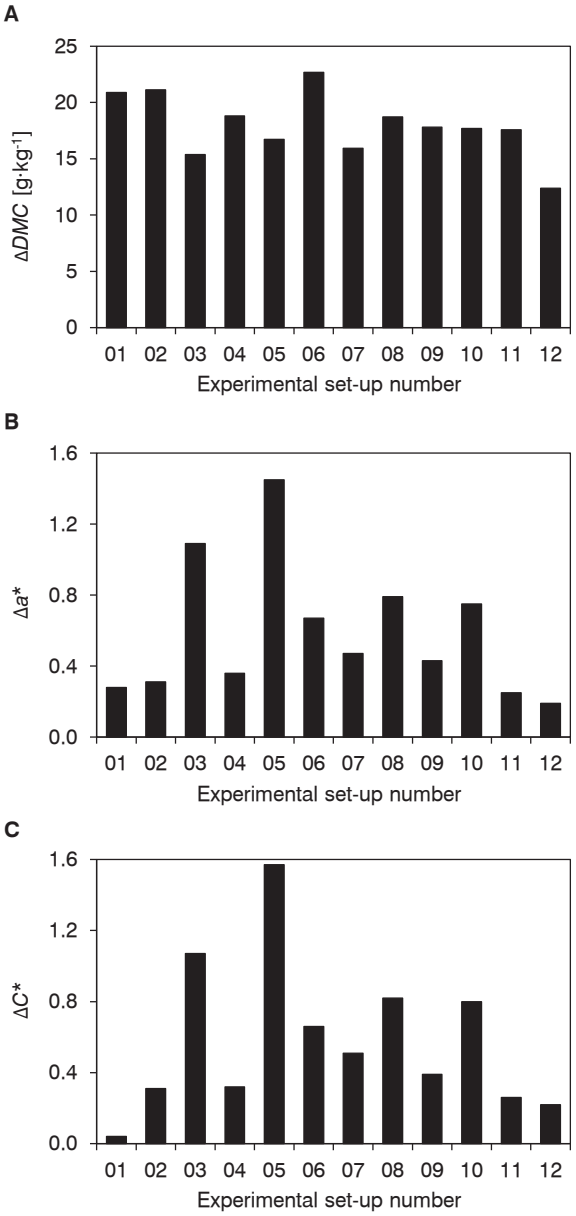

Fig. 2. Differences of significant physico-chemical parameters between the membrane separated blood fractions of individual filtration experiment setups.

A – dry matter content (*DMC*), B – redness-greenness colour parameter (*a**), C – chroma (*C**).
Differences between retentate and permeate are given.

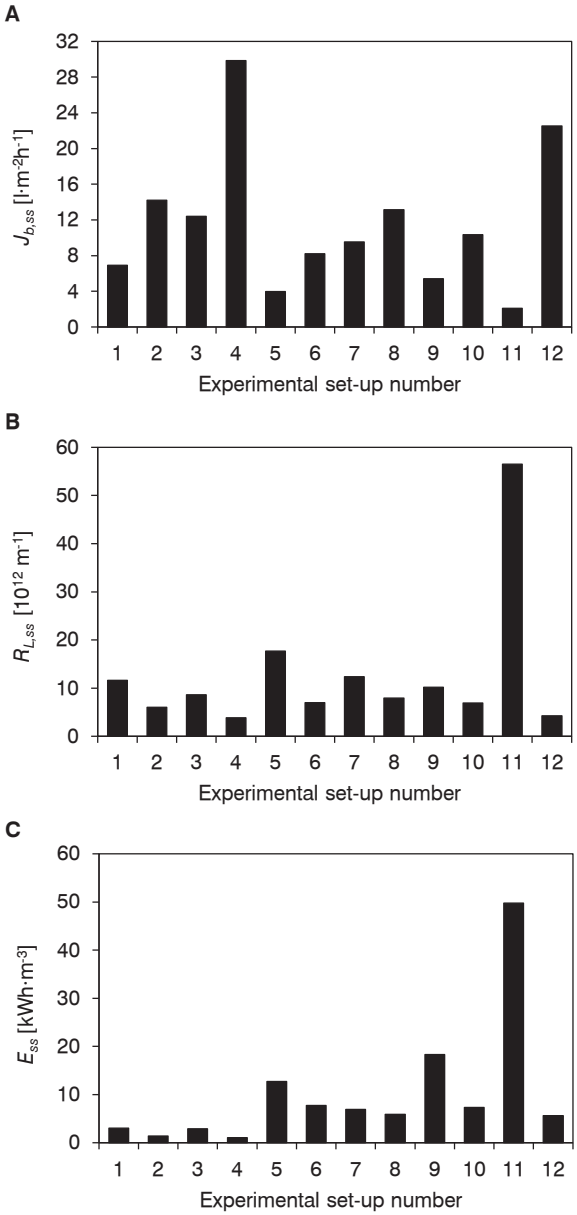

Fig. 3. The most important hydrodynamic and efficiency parameters of individual filtration experiment setups.

A – steady-state blood flux ($J_{b,ss}$), B – steady-state fouling layer resistance ($R_{L,ss}$), C – steady-state energy consumption (E_{ss}).

$p < 0.001$). All two-way and the three-way interactions were also highly significant ($p < 0.001$). The follow-up three-way univariate ANOVA with Bonferroni's adjustment revealed significance for all the variables a^*, C^* and dry matter content in case of all factors, namely, transmembrane pressure ($F(2;24) > 17.90$, $p < 0.001$), retentate flow rate ($F(1;24) > 38.80$, $p < 0.001$) and membrane pore size ($F(1;24) > 8.52$, $p < 0.001$). The difference between mean values of significant measured attributes of plasma and red blood cell fractions are presented in Fig. 2.

The best setup of the membrane separation from the 12 setups of the experimental plan was observed at transmembrane pressure of 2×10^5 Pa, retentate flow rate of 200 l·h^{-1} and membrane pore size of 1.2 μm in terms of blood product quality. The dry matter content of the red blood cell frac-

tion was the highest and chroma as well as red colour (a^* positive direction to red; a^* negative direction to green) related with the residual hemoglobin content and undesired sensory attributes of plasma fraction were among the lowest at this setting. This setup was the best in case of difference of dry matter content of blood products, because usually the clearest plasma and the most concentrated red blood cells are the most desirable for the industry.

Membrane filtration efficacy

The most important hydrodynamic and efficacy parameters of various filtration experiment setups (blood flux, steady-state fouling layer resistance, energy consumption) are shown in Fig. 3. In terms of efficacy, based on trend-like results, the best experimental setup for blood membrane separation was at 1×10^5 Pa transmembrane pressure, 300 $l \cdot h^{-1}$ retentate flow rate and 1.2 μm membrane pore size (setup 04) and the same experimental setup with 3×10^5 Pa (setup 12) was similarly good within the examined factor levels and experimental conditions. This can be explained by the fact that as the bigger membrane pore size, more cells and aggregates are allowed under 1×10^5 Pa transmembrane pressure, but 3×10^5 Pa transmembrane pressure with high retentate flow rate, which 'washes' the membrane's inner surface with the feed, pressing cells and aggregates through the membrane. Steady-state fouling layer resistance is grater in case of 0.8 μm membrane pore size and smaller in case of 1.2 μm membrane pore size, as well as globally lower in the case of lower transmembrane pressure. The practical flux stabilized after 10 min filtration time on 2.10–29.87 $l \cdot m^{-2} \cdot h^{-1}$. The filtration depends mostly on the previous parameter, because this flux characterizes most of the duration of industrial filtration.

Cleaning efficacy

The proposed cleaning method can be considered efficient because the average of flux recoveries was 101.9 % in case of 0.8 μm membrane pore size and 102.3 % in case of 1.2 μm membrane pore size. This can be explained by the fact that a lot of contamination adhered to the membrane before finding an effective washing protocol. This contamination was cleared continuously during the series of experiments. The difference between water flux values, which were measured before the experiments, was lower than 5 % and, therefore, the cleaning efficiency could be taken as sufficient.

Modelling

Parameter estimates, effect size estimates and significance of the regression coefficients from the Student's t-test of the significant parameters of the objective function are shown in Tab. 2. The standardized transmembrane pressure, the standardized membrane pore size and their interaction were involved in the model. The retentate flow rate together with its interactions with other factors had no significant effect on the steady-state fouling layer resistance. For this reason, the (standardized) retentate flow rate was eliminated from the model. Membrane pore size had significant effect on the steady-state fouling layer resistance, while transmembrane pressure and interaction of transmembrane pressure and membrane pore size had slightly significant effect on the dependent variable. Model accuracy and determination coefficients of the objective function were also significant: $F(3,8) = 5.683$, $p < 0.05$, multiple $R^2 = 0.68$, adjusted $R^2 = 0.56$. Lack of fit was insignificant ($F(2,6) = 0.66$, $p = 0.55$) and so the model was accepted. Optimization was carried out based on the model. The response surface of the effects of significant parameters for steady-state fouling layer resistance is shown in Fig. 4, which

Tab. 2. Parameter (coefficient) estimates and effect size estimates of the significant parameters of the objective function.

	Coefficients				Effect size			
	Estimate	Standard error	*t* value	*Pr* (>|t|)	Estimate	Standard error	*t* value	*Pr* (>|t|)
Intercept	10.20×10^{12}	2.56×10^{12}	4.00	< 0.01 ***				
TMP	9.09×10^{12}	3.14×10^{12}	2.90	< 0.05 **	0.6792	0.2211	3.072	< 0.050 **
MPS	-5.38×10^{12}	2.56×10^{12}	–2.10	0.07 *	–0.4024	0.1806	–2.229	0.053 *
TMP × *MPS*	-6.45×10^{12}	3.14×10^{12}	–2.06	0.07 *	–0.4825	0.2211	–2.182	0.057 *

Response was the steady-state fouling layer resistance.
TMP – transmembrane pressure, *MPS* – membrane pore size, *TMP* × *MPS* – interaction, *t* value – result of statistical test, *Pr* – level of significance (*** – $p < 0.01$, ** – $p < 0.05$, * – $p < 0.10$)

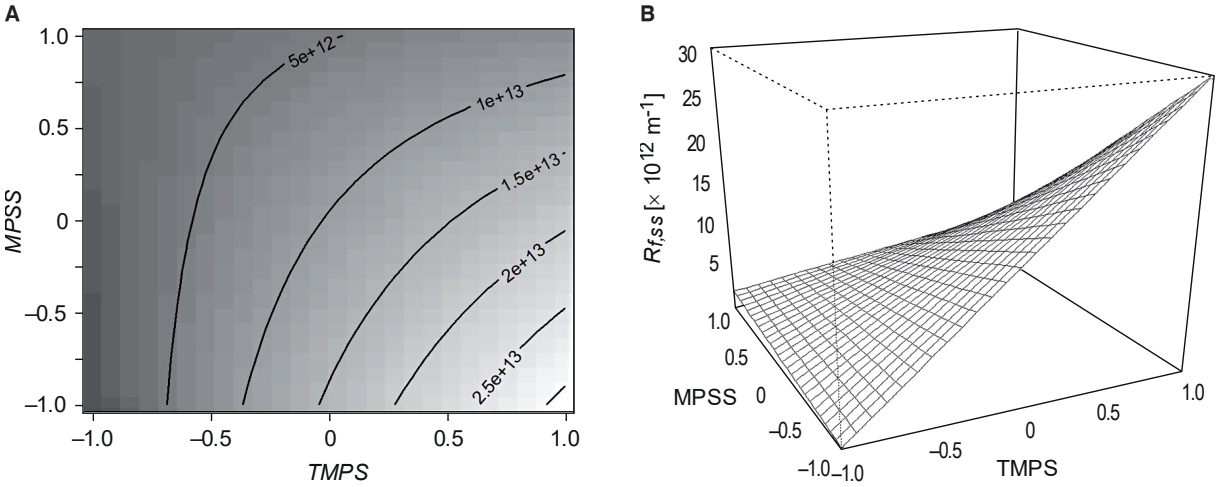

Fig. 4. Contour map and response surface of the effects of significant parameters for steady-state fouling layer resistance.

A – contour map; B – response surface.
TMPS – standardized transmembrane pressure, *MPSS* – standardized membrane pore size, $R_{f,ss}$ – steady-state fouling layer resistance.

also contains a two-dimensional contour map of the effects of significant parameters for steady-state fouling layer resistance. As can be seen in the figures, an optimum was found within the examined factor levels and experimental conditions. Therefore, the best (lowest) steady-state fouling layer resistance can be found at the lowest transmembrane pressure and largest membrane pore size.

CONCLUSIONS

Animal by-products, especially blood should be utilized as a raw material of food for the sustainability and for remedying existing global problems. There are good experiences with electrodialysis with ultrafiltration membrane for recovering bioactive peptides from animal blood as well as plant-based materials [37, 38], but very limited information was available on the basic separation by microfiltration. The methodology of porcine blood membrane separation was found to be appropriate. Valuable information was collected about the effect of filtration parameters (transmembrane pressure, membrane pore size, retentate flow rate) for physical and chemical parameters (rheological parameters, dry matter content, colour parameters, water activity, pH) of blood products (plasma, red blood cells) gained from filtration. The experimental design was analysed, parameters of the objective function and effect sizes were estimated and the global minimum of the objective function was successfully determined. The membrane separation parameters were optimized according to the model based on observation, with the optimum being found within the examined factor levels and experimental conditions. The efficacy of the membrane cleaning method appropriate for this specific purpose was found adequate. Remarkably, a single tubular membrane module was used during all experiments, so filtration efficiency can be increased in the case of scaling. According to the analysis of the experimental design, the transmembrane pressure and the membrane pore size had significant effects on the steady-state fouling layer resistance. No other significant effect was found in the case of retentate flow rate, which is very important because the retentate flow rate can be set at the best option for the energy consumption under such flow conditions within the examined factor levels. The lowest steady-state fouling layer resistance, thereby, the best filtration efficiency, was observed and calculated at the lowest transmembrane pressure and largest membrane pore size. Based on our results, adequate parameters can be selected for blood separation in case of producing primarily specific quality plasma as well as the red blood cell fraction. The quality of plasma fraction usually depends on colour (redness/greenness and chroma) and clearness (dry matter content), meanwhile the quality of red blood cells fraction usually depends on iron content, which is related to a^* (redness/greenness) and chroma, and dry matter content. So, the optimal setup is usually the same as the one in terms of

blood product quality. The optimal setup of blood product quality and optimal setup of efficiency are different. The difference between product quality of two optimal setups is relatively small. However, their colour deviance is barely perceptible to the human eye. This difference of energy consumption is an order of magnitude measured in kilowatthour per cubic meter dimension.

The methodology of blood membrane separation and membrane cleaning we introduced in this paper can be implemented for product and technology development and, after the experiments presented in this paper, can be scaled up by the industry. Membrane separation may become the next applied process utilized for the varied uses of blood in several enrichment procedures due to the controllability of product quality and relatively low resource demand with the adequate filtration volume.

Acknowledgements

This work was supported by the Hungarian University of Agriculture and Life Sciences, Doctoral School of Food Sciences (Budapest, Hungary). Authors are grateful to Edit Márki, a post-humous co-author of this paper.

REFERENCES

1. Floros, J. D. – Newsome, R. – Fisher, W. – Barbosa-Cánovas, G. V. – Chen, H. – Dunne, C. P. – German, J. B. – Hall, R. L. – Heldman, D. R. – Karwe, M. V. – Knabel, S. J. – Labuza, T. P. – Lund, D. B. – Newell-McGloughlin, M. – Robinson, J. L. – Sebranek, J. G. – Shewfelt, R. L. – Tracy, W. F. – Weaver, C. M. – Ziegler, G. R.: Feeding the world today and tomorrow: the importance of food science and technology. Comprehensive Reviews in Food Science and Food Safety, *9*, 2010, pp. 572–599. DOI: 10.1111/j.1541-4337.2010.00127.x.
2. Harwatt, H. – Sabaté, J. – Eshel, G. – Soret, S. – Ripple, W.: Substituting beans for beef as a contribution toward US climate change targets. Climatic Change, *143*, 2017, pp. 261–270. DOI: 10.1007/s10584-017-1969-1.
3. Gerber, P. J. – Steinfeld, H. – Henderson, B. – Mottet, A. – Opio, C. – Dijkman, J. – Falcucci, A. – Tempio, G.: Tackling climate change through livestock: A global assessment of emissions and mitigation opportunities. Rome : Food and Agriculture Organization of the United Nations, 2013. ISBN: 978-92-5-107920-1. <https://www.fao.org/3/i3437e/i3437e.pdf>
4. Godfray, H. C. J. – Beddington, J. R. – Crute, I. R. – Haddad, L. – Lawrence, D. – Muir, J. F. – Pretty, J. – Robinson, S. – Thomas, S. M. – Toulmin, C.: Food security: the challenge of feeding 9 billion people. Science, *327*, 2010, pp. 812–818. DOI: 10.1126/science.1185383.
5. Boland, M. J. – Rae, A. N. – Vereijken, J. M. – Meuwissen, M. P. – Fischer, A. R. – van Boekel, M. A. – Rutherfurd, S. M. – Gruppen, H. – Moughan, P. J. – Hendriks, W. H.: The future supply of animal-derived protein for human consumption. Trends in Food Science and Technology, *29*, 2013, pp. 62–73. DOI: 10.1016/j.tifs.2012.07.002.
6. Livestock's long shadow: environmental issues and options. Rome : Food and Agriculture Organisation of the United Nations, 2006. ISBN: 978-92-5-105571-7. <https://www.fao.org/3/a0701e/a0701e.pdf>
7. McGuire, S.: FAO, IFAD, and WFP. The state of food insecurity in the world 2015: meeting the 2015 international hunger targets: taking stock of uneven progress. Rome: FAO, 2015. Advances in Nutrition, *6*, 2015, pp. 623–624. DOI: 10.3945/an.115.009936.
8. Miller, J. L.: Iron deficiency anemia: a common and curable disease. Cold Spring Harbor Perspectives in Medicine, *3*, 2013, a011866. DOI: 10.1101/cshperspect.a011866.
9. Ockerman, H. W. – Hansen, C. L.: Animal by-product processing and utilization. Boca Raton : CRC Press, 2000. ISBN: 9780429179853. DOI: 10.1201/9781482293920.
10. Sorapukdee, S. – Narunatsopanon, S.: Comparative study on compositions and functional properties of porcine, chicken and duck blood. Korean Journal for Food Science of Animal Resources, *37*, 2017, pp. 228–241. DOI: 10.5851/kosfa.2017.37.2.228.
11. FoodData Central search results. In: U.S. Department of Agriculture – Agricultural Research Service [online]. Washington, D.C. : U.S. Department of Agriculture, 2018 [accessed 2018]. <https://fdc.nal.usda.gov/fdc-app.html#/>
12. Vitamin and mineral requirements in human nutrition : report of a Joint FAO-WHO Expert Consultation, Bangkok, Thailand, 21–30 September 1998. 2nd edition. Geneva : World Health Organization, 2004. ISBN: 9241546123.
13. Ofori, J. A. – Hsieh, Y. H. P. (Ed).: The use of blood and derived products as food additives. In: Food additives. Rijeka : IntechOpen, 2012, pp. 230–256. ISBN: 978-953-51-0067-6. DOI: 10.5772/32374.
14. Toldrá, F. – Aristoy, M. C. – Mora, L. – Reig, M.: Innovations in value-addition of edible meat by-products, Meat Science, *92*, 2012, pp. 290–296. DOI: 10.1016/j.meatsci.2012.04.004.
15. Bah, C. S. – Bekhit, A. E. D. A. – Carne, A. – McConnell, M. A.: Slaughterhouse blood: an emerging source of bioactive compounds. Comprehensive Reviews in Food Science and Food Safety, *12*, 2013, pp. 314–331. DOI: 10.1111/1541-4337.12013.
16. Regulation (EC) No 853/2004 of the European Parliament and of the Council of 29 April 2004 laying down specific hygiene rules for food of animal origin. Official Journal of European Communities, *47*, 2004, L139, pp. 55–205. ISSN: 1725-2555. <http://data.europa.eu/eli/reg/2004/853/oj>
17. Boyaci-Gündüz, C. P. – Ibrahim, S. A. – Wei, O. C. – Galanakis, C. M.: Transformation of the food sector: Security and resilience during the COVID-19 pandemic. Foods, *10*, 2021, article 497. DOI: 10.3390/

foods10030497.
18. Galanakis, C. M.: Separation of functional macromolecules and micromolecules: from ultrafiltration to the border of nanofiltration. Trends in Food Science and Technology, *42*, 2015, pp. 44–63. DOI: 10.1016/j.tifs.2014.11.005.
19. Galanakis, C. M.: The food systems in the era of the coronavirus (COVID-19) pandemic crisis. Foods, *9*, 2020, article 523. DOI: 10.3390/foods9040523.
20. Galanakis, C. M. – Aldawoud, T. – Rizou, M. – Rowan, N. J. – Ibrahim, S. A.: Food ingredients and active compounds against the coronavirus disease (COVID-19) pandemic: a comprehensive review. Foods, *9*, 2020, article 1701. DOI: 10.3390/foods9111701.
21. Galanakis, C. M.: Functionality of food components and emerging technologies. Foods, *10*, 2021, article 128. DOI: 10.3390/foods10010128.
22. Galanakis, C. M. – Rizou, M. – Aldawoud, T. M. – Ucak, I. – Rowan, N. J.: Innovations and technology disruptions in the food sector within the COVID-19 pandemic and post-lockdown era. Trends in Food Science and Technology, *110*, 2021, pp. 193–200. DOI: 10.1016/j.tifs.2021.02.002.
23. Regulation (EC) No 1333/2008 of the European Parliament and of the Council of 16 December 2008 on food additives. Official Journal of European Communities, *51*, 2008, L354, pp. 16–33. ISSN: 1725-2555. <http://data.europa.eu/eli/reg/2008/1333/oj>
24. Makara, A. – Kowalski, Z. – Fela, K. – Generowicz, A.: Utilization of animal blood plasma as example of using cleaner technologies methodology. Technical transactions, *1-Ś*, 2016, pp. 87–96. DOI: 10.4467/2353737XCT.16.197.5946.
25. Ananey-Obiri, D. – Matthews, L. – Azahrani, M. H. – Ibrahim, S. A. – Galanakis, C. M. – Tahergorabi, R.: Application of protein-based edible coatings for fat uptake reduction in deep-fat fried foods with an emphasis on muscle food proteins. Trends in Food Science and Technology, *80*, 2018, pp. 167–174. DOI: 10.1016/j.tifs.2018.08.012.
26. Li, K.: Ceramic membranes for separation and reaction. Chichester : John Wiley & Sons, 2007. ISBN: 9780470014400.
27. Galanakis, C. M.: Sustainable applications for the valorization of cereal processing by-products. Foods, *11*, 2022, article 241. DOI: 10.3390/foods11020241.
28. Mezger, T. G.: The rheology handbook: for users of rotational and oscillatory rheometers. 3rd revised edition. Hannover : Vincentz Network, 2006. ISBN: 978-3-86630-890-9.
29. Liu, J. – Tan, Y. – Zhou, H. – Mundo, J. L. M. – McClements, D. J.: Protection of anthocyanin-rich extract from pH-induced color changes using water-in-oil-in-water emulsions. Journal of Food Engineering, *254*, 2019, pp. 1–9. DOI: 10.1016/j.jfoodeng.2019.02.021.
30. Gaspar, I. – Koris, A. – Bertalan, Z. – Vatai, G.: Comparison of ceramic capillary membrane and ceramic tubular membrane with inserted static mixer. Chemical Papers, *65*, 2011, pp. 596–602. DOI: 10.2478/s11696-011-0045-y.
31. Xie, F. – Chen, W. – Wang, J. – Liu, J.: CFD and experimental studies on the hydrodynamic performance of submerged flat-sheet membrane bioreactor equipped with micro-channel turbulence promoters. Chemical Engineering and Processing: Process Intensification, *99*, 2016, pp. 72–79. DOI: 10.1016/j.cep.2015.10.012.
32. Ben Hassan, I. – Ennouri, M. – Lafforgue, C. – Schmitz, P. – Ayadi, A.: Experimental study of membrane fouling during crossflow microfiltration of yeast and bacteria suspensions: Towards an analysis at the microscopic level. Membranes, *3*, 2013, pp. 44–68. DOI: 10.3390/membranes3020044.
33. Blanpain-Avet, P. – Migdal, J. F. – Bénézech, T.: The effect of multiple fouling and cleaning cycles on a tubular ceramicmicrofiltration membrane fouled with a whey protein concentrate: Membrane performance and cleaning efficiency. Food and Bioproducts Processing, *82*, 2004, pp. 231–243. DOI: 10.1205/fbio.82.3.231.44182.
34. Sun, Y. – Qin, Z. – Zhao, L. – Chen, Q. – Hou, Q. – Lin, H. – Jiang, L. – Liu, J. – Du, Z.: Membrane fouling mechanisms and permeate flux decline model in soy sauce microfiltration, Journal Food Process Engineering, *41*, 2018, e12599. DOI: 10.1111/jfpe.12599.
35. Varga, A. – Ladányi, M. – Márki, E.: Modeling of beer membrane filtration. Desalination and Water Treatment, *192*, 2020, pp. 382–391. DOI: 10.5004/dwt.2020.25460.
36. Lenth, R. V.: Response-surface methods in R, using rsm. Journal of Statistical Software, *32*, 2010, pp. 1–17. DOI: 10.18637/jss.v032.i07.
37. Przybylski, R. – Bazinet, L. – Firdaous, L. – Kouach, M. – Goossens, J. F. – Dhulster, P. – Nedjar, N.: Harnessing slaughterhouse by-products: From wastes to high-added value natural food preservative. Food Chemistry, *304*, 2020, article 125448. DOI: 10.1016/j.foodchem.2019.125448.
38. González-Montoya, M. – Hernández-Ledesma, B. – Mora-Escobedo, R. – Martínez-Villaluenga, C.: Bioactive peptides from germinated soybean with anti-diabetic potential by inhibition of dipeptidyl peptidase-IV, α-amylase, and α-glucosidase enzymes. International Journal of Molecular Sciences, *19*, 2018, article 2883. DOI: 10.3390/ijms19102883.

Received 15 March 2022; 1st revised 31 May 2022; accepted 1 June 2022; published online 18 July 2022.